Bulletin of Earthquake Engineering (2025) 23:2537–2556
https://doi.org/10.1007/s10518-025-02120-1

ORIGINAL ARTICLE

Proposal of horizontal elastic response spectra for low and high seismicity regions towards the revision of Algerian seismic code

Nasser Laouami[1] · **Abdennasser Slimani**[1]

Received: 1 August 2024 / Accepted: 2 February 2025 / Published online: 21 March 2025

Abstract
The elastic response spectra are fundamental engineering tools provided by seismic codes for performing structural seismic analysis and seismic risk reduction. This work is performed in the framework of the ongoing revision of the current Algerian seismic code RPA99/2003, which provides elastic spectra whose reproduction performance of real seismic actions, is called into question by recent earthquakes. Algerian seismicity is characterized by frequent moderate earthquakes, as well as rare severe earthquakes such as those of Boumerdes (Mw = 6.8 on May 21, 2003) and El Asnam (Ms = 7.3 on October 10, 1981). The compilation of a large accelerometric database from Algeria and the surrounding areas has recently made it possible to develop new horizontal elastic acceleration response spectra and soil amplification factors for four different soil classes— very soft, soft, firm, and rock—as well as for two seismicity levels—weak to moderate seismicity (wms) for the central and southern regions and moderate to high seismicity (mhs) for the northern region. 153 earthquakes are used, with a total of 773 3-component records from events with magnitudes ranging from 3.0 to 7.4 and hypocentral distances less than 200 Km. A statistical approach is used which leads to the estimation of new constant spectral acceleration branch limits and soil factors for the proposed horizontal elastic response spectra, for two seismicity levels and four soil classes. Soil factors for the two seismicity levels are estimated using the intensity of the Housner spectrum. Significant variations in elastic spectra developed for the two seismicity levels, wms and mhs, are highlighted. The first difference involves the branch plateau of the constant spectral acceleration, which swings toward the high periods in mhs but is dominated by the low periods in wms. The second difference is the spectrum amplitude related to site factors, which is less important in the case of mhs due to the effects of nonlinearities in soils subjected to strong seismic accelerations. Furthermore, comparing the proposed elastic acceleration spectra with the spectra provided by Pitilakis et al. (2018), developed in the framework of the ongoing revision of Eurocode 8, reveals comparable trends.

Keywords Elastic response spectra · Seismic design code · Strong motion database · Soil factors, RPA

Extended author information available on the last page of the article

1 Introduction

Engineers can use response spectra to quantify the demands of earthquake ground motion on the capacity of buildings to resist earthquakes. In general, the response spectrum is jagged, with sharp peaks and valleys, and is represented as acceleration response spectra or displacement response spectra. Housner (1959) was the first to create smoothed mean standard spectral shapes from the horizontal components of four accelerograms recorded in El Centro, California, in 1934 and 1940; Olympia, Washington, in 1949; and Taft, California, in 1952.

To develop probabilistic design spectra, methods of constructing smooth response spectra for design purposes have been developed, such as the use of a constant acceleration for short period responses, a constant velocity for the mid-range, and a constant displacement for long period responses (Newmark and Hall 1982).

Following destructive earthquakes, seismic codes are revised and updated to reflect advances in knowledge. On the framework of the ongoing revision of Eurocode 8 seismic code (CEN 2004), Pitilakis et al. (2018) proposed an alternative site classification scheme and associated dependent spectral amplification factors. A comprehensive worldwide database of strong ground motion records from sites, which dispose a very well-documented soil down to seismic bedrock (Vs > 800 m/s), is used. The important improvements concern the introduction of the fundamental period of the site and sub-classes for the soil classes B and C of the Eurocode 8; the use of two anchoring spectral values, for short and intermediate periods and the upper corner period depending on the local seismic hazard; the scalar intensity variation of site amplification factors, for each soil and site category, to account for soil nonlinearity. Harmon et al. (2019a, b) developed site amplification models for Central and Eastern North America. Based on robust parametric study of 1-D ground response analyses, they developed linear and non-linear site amplification functions by considering the effect of time-averaged 30 m shear wave velocity (Vs_{30}, site period, sediment depth and non-linearity of soil. Deoda and Adhikary (2020) worked on the improvement of the site classification scheme and amplification factors for the Indian seismic code (2020). Based on numerical computations, they propose a new normalized acceleration response spectra as well as period dependent soil amplification factors.

Northern Algeria lies along the Africa-Eurasia plate boundary. It is one of the most seismically active areas in the western Mediterranean. The seismicity distribution is represented by four (04) seismic areas (RPA99/2003 2003), seismic zones IIb and III for moderate to high seismicity (mhs), and I and IIa for weak to moderate seismicity (wms) (Fig.1). Several moderate-to-strong earthquakes struck northern Algeria over the last three decades, with two of them causing significant damage. The 1980 El Asnam earthquake (M7.3), which killed over 2700 people and destroyed approximately 60,000 homes, and Boumerdes May 21 (M6.8) caused significant damage and killed over 2300 people. Knowing that earthquake-resistant design is the most effective way to reduce seismic risk, the Algerian government issued the first Algerian seismic regulation, RPA81, shortly after the 1980 El Asnam devastating earthquake (M7.3). This document was revised in 1988, 1999, and 2003, just after the devastating Boumerdes earthquake (M6.8), and it is currently being revised.

The current study investigates the accuracy of Algerian horizontal elastic response spectra and soil factors S for different soil classes proposed in RPA99/2003 (2003) using a large database of ground motion records from Algeria and surrounding regions, which was

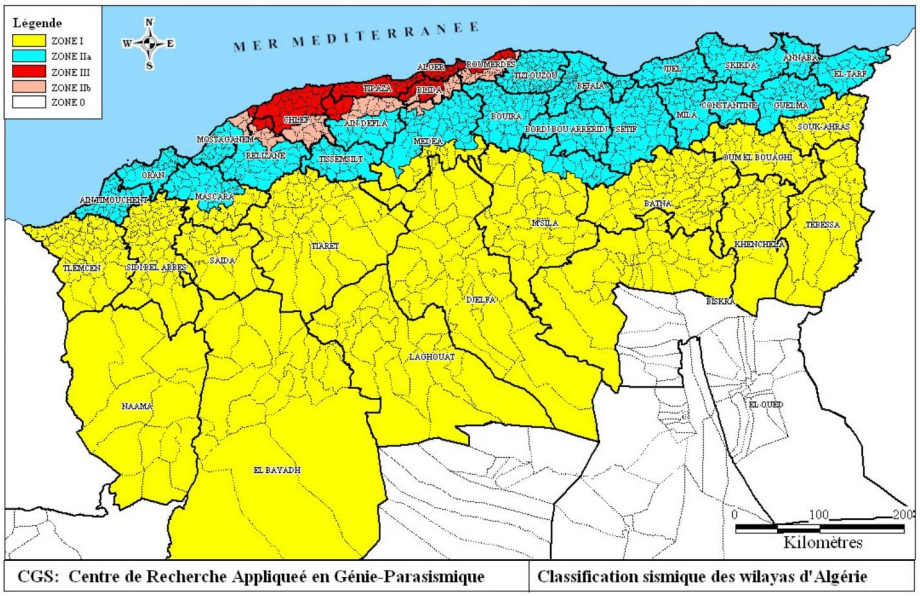

Fig. 1 Algerian seismic zoning map (RPA99/2003 2003)

recently used to develop ground motion prediction equation for Algeria (Laouami et al. 2018a). The main goal is to propose improved parameters and normalized shapes for the Algerian seismic code's horizontal elastic response spectra, which could be included in the ongoing revised version.

1.1 Review of the Algerian elastic design spectra

RPA99-2003 (2003) defines the elastic response spectrum for four (04) main soil classes S_1, S_2, S_3 and S_4. When available, the mean shear wave velocity over 30 m V_{s30} should be used for site classification; otherwise, one of the following parameters should be used: the static penetrometer average peak resistance q_c, the standard penetration test blow-count N_{SPT}, the average limit pressure P, the average pressure module E_p, and the simple compressive strength q_u (Table 1). The classification criteria in Table 1 are related to the stratigraphic profile description.

The shape of response spectra is affected by a variety of seismological and geophysical parameters. Many authors (Ambraseys et al. 1996; Bommer and Acevedo 2004) presented and discussed how earthquake magnitude, source-to-site distance, and site classification affect response spectra. In the current version of the Algerian seismic code (RPA99/2003 2003), only the effect of soil class through the lower and the upper limits of the period of the constant spectral acceleration branch is included in the definition of elastic design spectra. The seismicity level effect and the soil factors are not incorporated in the current definition.

Equation (1) to (4) and the parameters listed in Table 2 give the horizontal elastic design spectra for 4 subsoil classes. T1 and T2 show the lower and the upper limits of the period of the constant spectral acceleration branch, and T = 3 s shows the value defining the beginning

Table 1 Soil classes defined in RPA99-2003 (2003)

Soil class	Description	q_c (MPa)	N	P (MPa)	E_p (MPa)	q_u (MPa)	V_{s30} (m/s)
S_1	Rock or other geological formation	–	–	> 5	> 100	> 10	≥ 800
S_2	Very dense deposits of sand and gravel and / or overconsolidated clay 10 to 20 m thick with $V_s \geq$ 400 m/s from 10 m deep	> 15	> 50	2–5	20–100	0.4–10	400–800
S_3	Thick deposits of medium dense sands and gravels or medium rigid clay with $V_s \geq$ 200 m/s from 10 m deep	1.5–15	10–50	1–2	5–20	0.1–0.4	200–400
S_4	Deposits of loose sand with or without the presence of soft clay layers with V_s <200 m/s in the first 20 m	< 1.5	< 10	< 1	< 5	< 0.1	100–200

Table 2 Ordinates of elastic design spectra for RPA99-2003 (2003)

Soil Class	S1	S2	S3	S4
T1 (sec)	0.15	0.15	0.15	0.15
T2 (sec)	0.30	0.40	0.50	0.70
Soil factor	1	1	1	1

of the constant displacement response range of the spectrum, η is the damping correction factor, with a reference value $\eta = 1$ for 5% damping ratio, and a_g is the peak ground acceleration corresponding to a period T = 0. Figure 2 shows the currently used Algerian design elastic response spectra.

$$S_a(g) = \begin{cases} 1.25a_g\left(1 + \frac{T}{T_1}(2.5\eta - 1)\right) & 0 \leq \mathrm{T} < \mathrm{T}_1 \quad (1) \\ 2.5\eta\,(1.25a_g) & \mathrm{T}_1 \leq \mathrm{T} < \mathrm{T}_2 \quad (2) \\ 2.5\eta\,(1.25a_g)\left(\frac{T_2}{T}\right)^{2/3} & \mathrm{T}_2 \leq \mathrm{T} < 3\mathrm{s} \quad (3) \\ 2.5\eta\,(1.25a_g)\left(\frac{T_2}{3}\right)^{2/3}\left(\frac{3}{T}\right)^{5/3} & \mathrm{T} > 3\mathrm{s} \quad (4) \end{cases}$$

1.2 Strong motion database and site classification

In this study, 153 earthquakes are used, with a total of 773 3-component records from events with magnitudes ranging from 3.0 to 7.4 and hypocentral distances less than 200 Km. The Algerian strong motion database managed by CGS provides 614 horizontal records, the European strong motion database (Ambraseys et al. 2000) provides 774 horizontal records, and the USGS and the California Division of Mines and Geology (CDMG) strong motion databases provides 158 horizontal records. Figure 3 illustrates the record distribution as a function of magnitude and hypocentral distance. The M-R distribution emphasizes an interesting contribution of different magnitude and distance intervals, and thus it is appropriate for the development of elastic design spectra for different magnitude levels. All data come from shallow crustal earthquakes and reverse faults in active regions (e.g., western North America, Italy, Algeria, Greece, and so on) with depths less than 30 km, which corresponds to the Algerian seismotectonic context.

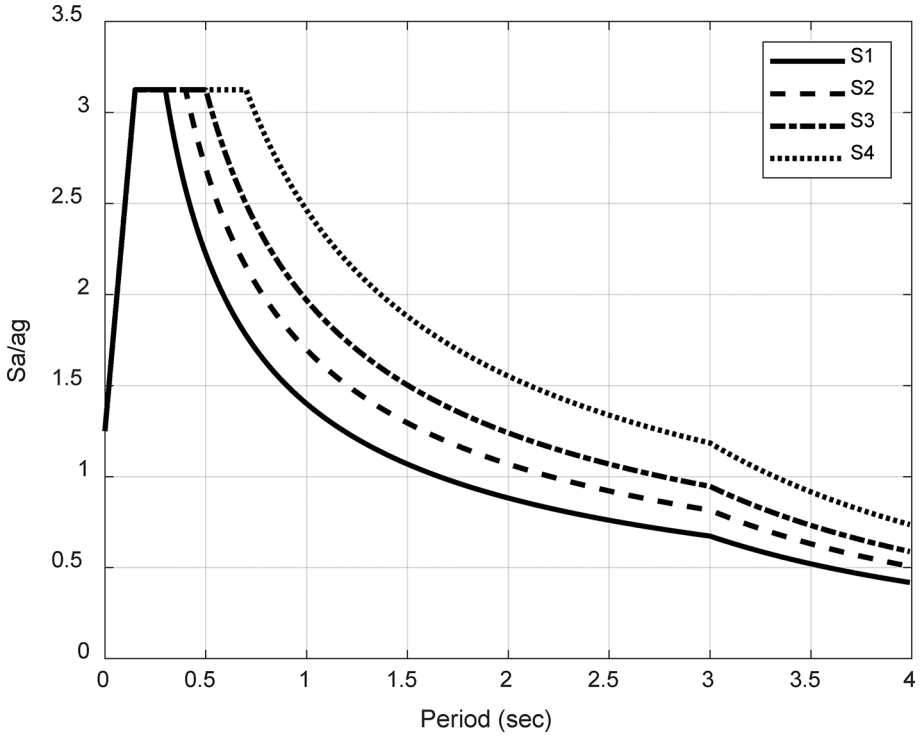

Fig. 2 Algerian design elastic response spectra (RPA99/2003 2003)

The strong motion database has been divided into two subgroups according to the magnitude. The first subgroup covers all earthquake records with magnitude M > 5.5 (mhs). It allows elaborating the seismicity level 1 spectra. The second subgroup covers all earthquake records with magnitude M <= 5.5 (wms). It allows elaborating the seismicity level 2 spectra. This subdivision of the database into magnitude classes allows normalizing the spectra with regard to seismic hazard.

The recording stations are classified using the soil classification scheme developed by Laouami et al. (2018b) (Laouami 2020), according to the soil-classification criteria in Table 3. It defines target horizontal over vertical spectral ratios (Laouami et al. 2018b), hv_{tar} (Fig. 4), for the four soil classes specified in Table 3. The intersection between the four target HVSRs define the frequency ranges for the four soil classes. This classification relies on matching the recorded strong motion H/V spectral ratio with one of the 04 hv_{tar} defined for each of the 4 soil classes as follows:

i. Subdivide the 03-components record (E-W, N-S, and Z) into 90-percent overlapping 10-second windows, yielding N temporal windows. The HVSR of each window is calculated as the geometric average of both horizontal component spectra divided by the vertical spectrum (Eq. 5), referred hereafter hv_{win}.

$$hv_{win}(f) = \frac{\sqrt{RS_{win,ew}(f).RS_{win,ns}(f)}}{RS_{win,ver}(f)} \tag{5}$$

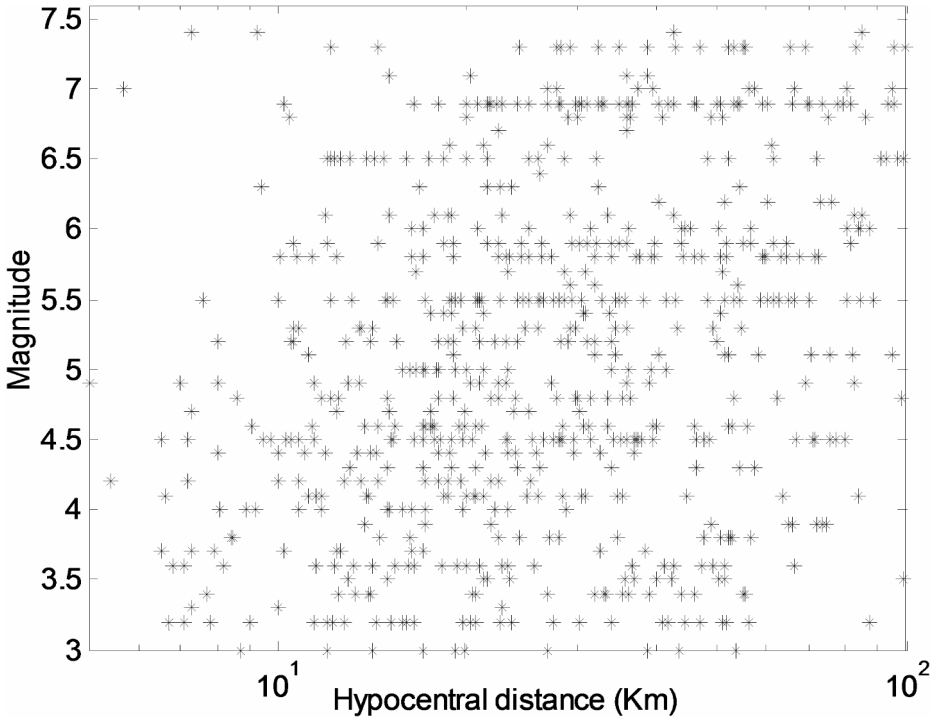

Fig. 3 Distribution of the records as a function of magnitude and hypocentral distance

Table 3 Definition of the soil classes based on shear wave velocity used in Laouami et al. (Laouami 2020) and the corresponding Algerian code RPA99/2003 (2003) soil classes

Soil class	Soil profile	Shear wave velocity (m/s)	RPA99/2003 (2003)
SCA	Rock	>800	S1
SCB	Very dense soil and soft rock	360–800	S2
SCC	Stiff soil	180–360	S3
SCD	Soft soil	100–180	S4

with $RS_{win,ew}(f)$, $RS_{win,ns}(f)$, and $RS_{win,ver}(f)$ are the time window elastic response spectra of the east-west, north-south and vertical components respectively, for a damping coefficient of 5%.

- Classify each of the N temporal windows by calculating the Site Classification Index (SI) given by Eq. 6. This involves comparing the calculated spectral ratio H/V for each temporal window, hv_{win},with each of the 4 target horizontal over vertical spectral ratios, hv_{tar} defined for the 4 soil classes. The soil class (SCA, SCB, SCC, and SCD) with the highest value of the Site Classification Index (SI) is assigned to the respective temporal window. Since the four targets hv_{tar} have various frequency intervals (Fig. 4), this strategy is one way to perform a frequency decomposition of the signal. An automated classification procedure has been developed for the N time windows.

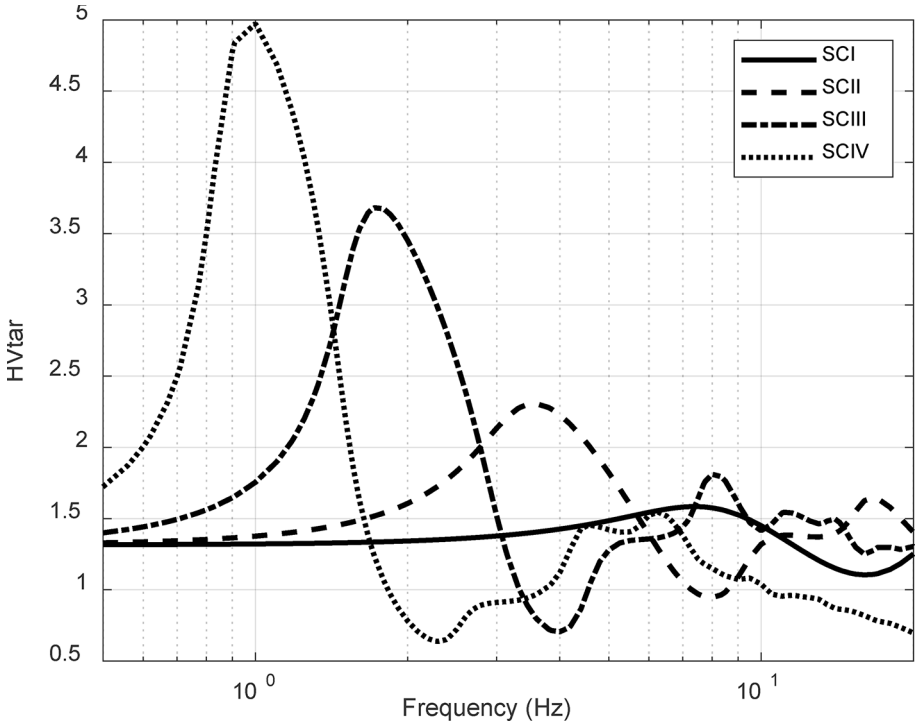

Fig. 4 Target analytical H/V spectral ratios, hv_{tar},for the four soil classes SCI, SCII, SCIII and SCIV

$$SI = \frac{R}{MQE} \tag{6}$$

where:

R is the correlation coefficient (Eq. 7), which measures the similarity between the spectral ratio H/V of the time window $hv_{win}$with each of the 4 target spectral ratios hv_{tar}.

$$\mathrm{R} = \frac{\mathrm{C}\left(\mathrm{hv_{tar}}\left(\mathrm{f}\right),\ \mathrm{hv_{win}}\left(\mathrm{f}\right)\right)}{\sqrt{\mathrm{C}\left(\mathrm{hv_{tar}}\left(\mathrm{f}\right),\ \mathrm{hv_{tar}}\left(\mathrm{f}\right)\right).\mathrm{C}\left(\mathrm{hv_{win}}\left(\mathrm{f}\right),\ \mathrm{hv_{win}}\left(\mathrm{f}\right)\right)}} \tag{7}$$

where.

$C\left(hv_{tar}\left(f\right),\ hv_{win}\left(f\right)\right) = E\left[hv_{tar}\left(f\right).hv_{win}\left(f\right)\right]$ is the covariance between hv_{tar} and hv_{win}, E is the mathematical expectation, $f$is the frequency in Hz, and N is the total number of frequencies.

MQE is the normalised mean squared error (Eq. 8), which is the amplitude difference between the spectral ratio H/V of the time window $hv_{win}$with each of the 4 target spectral ratios hv_{tar}.

$$MQE = \sqrt{\frac{1}{N}\left[\sum_{i=1}^{N}\left[\left(hv_{tar}\left(f_i\right) - hv_{win}\left(f_i\right)\right)^2 / \left(hv_{win}\left(f_i\right)\right)^2\right]\right]} \tag{8}$$

iii. The site classification principle is based on the following statistical criterion; the soil class with the maximum number of time windows is assigned to the considered site. This means that a higher number of time windows are characterized by vibration frequencies belonging to the elected soil class. The time windows assigned to the chosen soil class are used to calculate the mean H/V spectral ratio $\bar{hv}_{win}$ and the associated standard deviation, which provide the predominant frequency (f_g) corresponding to the largest peak of the $\bar{hv}_{win}$.

Table 4 displays the distribution of the strong motion database by soil and magnitude classes. It demonstrates a good distribution of 3-component records across the 4 soil classes, with 201, 287, 191, and 94 records for SCA, SCB, SCC, and SCD, respectively. Records from wms are more numerous because low magnitude earthquakes are the most frequent.

1.3 Normalized acceleration elastic response spectra

A smooth design spectrum should be developed under ideal conditions by using a large ensemble of strong-motion accelerograms with specified magnitude, distance, and geological condition. However, even with parameters close to the specified values, a sufficient number of accelerograms are not available in general. As a result, in order to obtain an averaged smooth response spectrum, the spectra of accelerograms recorded under widely varying conditions must be used. It is common practice to normalize each individual spectrum before averaging to remove the effects of variations in the controlling parameters.

To account for random scattering in the amplitudes of the spectra of real accelerograms, response spectra must be estimated with higher than mean confidence levels. This scattering can be attributed primarily to stochastic fluctuations in the amplitudes of recorded accelerograms, possible differences between reported and actual magnitude and distance values, and a qualitative description of the site condition. In the case of normalized standard spectra, the spectral shape of mean plus one standard deviation (σ) is used to account for random scattering in the observed data.

All available records (Table 4) were normalized to a value of unity at zero period and grouped into four soil classes and two seismicity levels. The median of these normalized spectra was calculated for each soil class and seismicity level, as well as the 16th and 84th percentiles, which represent the average minus and plus one standard deviation, respectively. Figure 5 depicts the normalized spectra (in grey) for the four soil classes and two seismicity levels, as well as the average and the average plus one standard deviation (in white). The normalized mean spectra shapes differ significantly between the soil and magnitude classes.

In Table 5, the values of the plateau amplitude (β in Eq. 9), which is the maximum of the normalized response spectra, are dressed for the four soil classes and two seismicity levels. The highest plateau amplitude is clearly shown for soil class SCA, with values of 2.8 for

Table 4 Distribution of the strong motion database with respect to soil class and magnitude class

Soil Category	SCA		SCB		SCC		SCD	
Magnitude class	mhs	wms	mhs	wms	mhs	wms	mhs	wms
Number of 3-component records	42	159	103	184	78	113	38	56
S/Total	201		287		191		94	
Total	773							

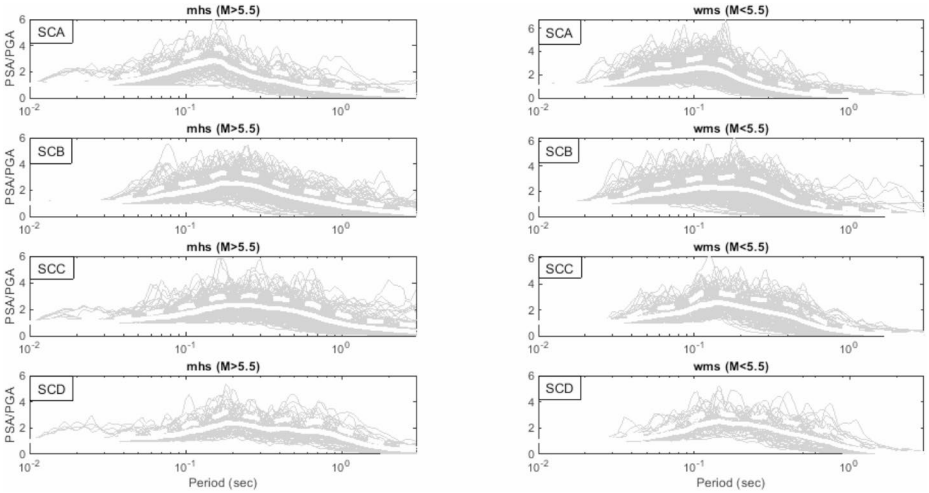

Fig. 5 The recorded horizontal PSA/PGA normalized spectral acceleration (in grey) for the 4 soil class and 2 seismicity levels, the median normalized spectral acceleration (solid white line), and the 84th (average plus one standard deviation, dashed white line) percentiles

Table 5 The values of the average amplitude of the plateau level (β in Eq. 9) for the 4 soil class and 2 seismicity levels, mhs and wms

Soil classes	SCA		SCB		SCC		SCD		Average β
Seismicity types	mhs	wms	mhs	wms	mhs	wms	mhs	wms	
Maximal amplitude of the average plateau level (β)	2.8	2.66	2.57	2.34	2.33	2.47	2.40	2.43	2.5

mhs, while the SCC and SCD soil classes show rather low values. However, the mean value of β, assumed in the following, is found to be 2.5.

1.4 Shape of horizontal elastic response spectra

Many related studies (Yang and Lee 2007; Moradpouri and Mojarab 2012) and seismic design codes (RPA99/2003 2003; CEN 2004; BSSC 1995) show that empirical trends of the elastic response spectra can be roughly divided into three parts: the ascent portion, the flat portion, and the decay portion. Equation (9) is the fitted general formula used to calibrate normalized horizontal response spectra in order to obtain the characteristic parameters.

$$S_e(T) = \begin{cases} a_g S \left[1 + \frac{T}{T_B}(\beta\,\eta - 1)\right] & 0 \le T \le T_B \\ \beta\, a_g S \eta & T_B \le T \le T_C \\ \beta\, a_g S \eta \left[\frac{T_C}{T}\right]^{\alpha} & T_C \le T \le T_D \\ \beta\, a_g S \eta \left[\frac{T_C T_D}{T^2}\right]^{\alpha} & T_D \le T \le 4s \end{cases} \tag{9}$$

where, $S_e(T)$ is the elastic response spectrum; T the vibration period of a linear single-degree-of-freedom system; a_g the design ground acceleration on soil type SCA scaled to 1; T_B and T_C are the limits of the constant spectral acceleration branch to be estimated by fitting the general form by the experimental normalized acceleration response spectra; T_D is the value defining the beginning of the constant displacement response range of the spectrum ($T_D = 2.0$ for seismicity level 1 and $T_D = 1.2$ for seismicity level 2); S is the soil factor scaled to 1; η is the damping correction factor, its reference value is $\eta = 1$ for 5% viscous damping, and β (set to 2.5 from Table 5) and α are the amplitude of the flat portion and attenuation index respectively.

The period interval where the PSA/PGA plateau (T_B-T_C) is constant is investigated in this section in order to propose standard shapes for the elastic response spectra using the strong motion database described in Table 4. Figure 6 depicts the recorded PSA/PGA normalized spectra (in grey) for each seismicity level (wms and mhs) and soil class (SCA, SCB, SCC, SCD), as well as the median normalized acceleration spectra (solid white line) and the 84th (average plus one standard deviation, dashed white line) percentiles. The first step consists to fit the 84th percentiles normalized acceleration spectra using the general formula (Eq. 9) to envelope the shape of the 84th percentiles normalized spectral acceleration at longer periods (dashed black line), accounting for as many uncertainties as possible.

The standard form of the proposed normalized acceleration response spectra (solid black line) is obtained from those obtained for the 84th percentiles (dashed black line) by setting the amplitude of the plateau equal to the average value of β=2.5. The limits of the constant spectral acceleration branch (T_B-T_C) are the intersections between the plateau and the standard form of the 84th percentile of the normalized acceleration spectra.

In Table 6, the period values of T_B and T_C obtained by the current study (in bold) are compared to those from the Algerian design code (RPA99/2003 2003), as well as the periods proposed by Pitilakis et al. (2013) in the context of improving the current EC8 soil classifi-

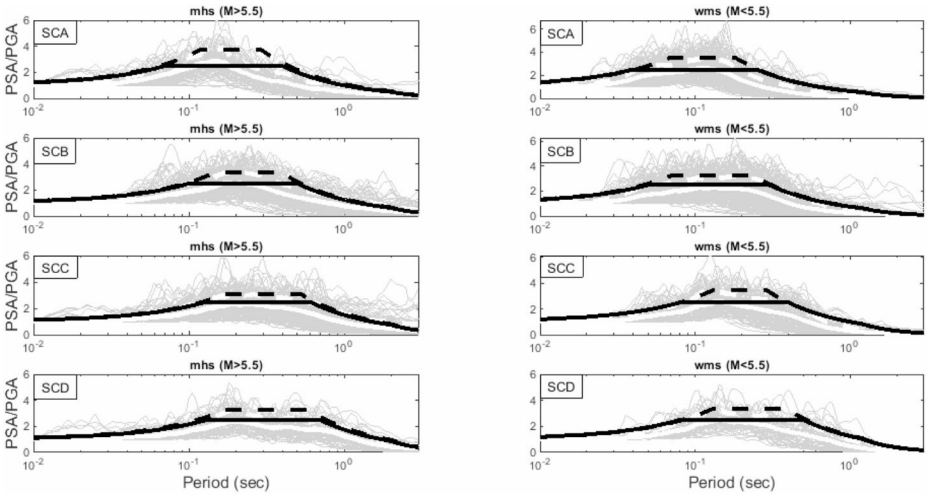

Fig. 6 The recorded horizontal PSA/PGA normalized spectral acceleration (in grey), the median normalized spectral acceleration (solid white line), and the 84th (average plus one standard deviation, dashed white line) percentiles, with the average (in black) and average plus one standard deviation (in dashed black line) derived elastic response spectra

Table 6 Comparison of the period values of T_B and T_C obtained by the present study with those from the Algerian design code RPA99/2003, and the periods proposed by Pitilakis et al. (2013), for the soil classes SCA, SCB, SCC and SCD and for the two category of seismicity wms and mhs

		This study		RPA99 (2003)		Pitilakis et al. (2013)*	
Soil Class	Magnitude Class	T_B	T_C	T_B	T_C	T_B	T_C
SCA	mhs	**0.10**	**0.40**	0.15	0.30	0.10	0.40
	wms	**0.05**	**0.25**			0.05	0.30
SCB	mhs	**0.10**	**0.50**	0.15	0.40	0.10	0.40–0.50 (0.45)
	wms	**0.05**	**0.30**			0.05	0.25–0.30 (0.28)
SCC	mhs	**0.15**	**0.60**	0.15	0.50	0.10	0.60-0.60-0.90 (0.70)
	wms	**0.10**	**0.40**			0.10	0.25–0.40-0.50 (0.38)
SCD	mhs	**0.15**	**0.70**	0.15	0.70	0.10	0.70
	wms	**0.10**	**0.50**			0.10	0.70

*Pitilakis et al. (2013) proposes 2 and 3 subclasses for SC-B and SC-C respectively (the average value is given in brackets)

Table 7 Number of strong motion records for each magnitude interval and seismicity class

Soil	wms				mhs			
Class	3.5<M≤4	4<M≤4.5	4.5<M≤5	5<M≤5.5	5.5<M≤6	6<M≤6.5	6.5<M≤7	7<M≤7.5
SCA	106	30	56	32	46	18	**14**	**6**
SCB	84	58	72	64	80	32	58	24
SCC	60	42	48	34	76	22	58	26
SCD	**12**	24	32	**10**	28	**6**	26	**10**

cation using a worldwide database of strong ground motion records, for the soil classes A, B, C, and D, and for the two seismicity levels mhs and wms.

The results show the limits of the constant spectral acceleration branch (T_B-T_C) shift to higher periods when the magnitude changes from wms ($M \leq 5.5$) to mhs ($M > 5.5$). This result supports our interest in proposing two types of spectra (wms and mhs) for the two seismicity levels. The comparison also reveals that the Algerian design code overestimates the period T_B and underestimates T_C, as compared with the proposed elastic spectra. A comparison with the periods of Pitilakis et al. (2013) reveals a similar trend.

1.5 Soil factor of horizontal elastic response spectra

It is widely accepted that soil factor represents the amplification of ground motion caused by the presence of subsoil layers in relation to geological bedrock. As a result, soil factor S for subsoil class SCA is set to 1.0; in this work, we computed soil factor of horizontal elastic response spectra using intensity-based soil factors proposed by Rey et al. (2002). For each seismicity class, the strong motion database is divided into four magnitude ranges ($3.5 < M \leq 4.0$, $4.0 < M \leq 4.5$, $4.5 < M \leq 5.0$, $5.0 < M \leq 5.5$ for wms, and $5.5 < M \leq 6.0$, $6.0 < M \leq 6.5$, $6.5 < M \leq 7.0$, $7.0 < M \leq 7.5$ for mhs). The number of strong motion records for each magnitude interval and seismicity class is shown in Table 7. Overall, the number of records per subclass appears to be representative, with the exception of soil class SCD, which has a lower number of records.

The hypocentral distance R was multiplied by the spectral ordinates $S_a(T)$. The evidence of attenuation relations, which show that response spectral accelerations are consis-

tently proportional to distance elevated to an exponent close to −1, supports such distance normalization. As a result, the shapes of spectra do not change noticeably with distance (Rey et al. 2002). The Housner spectrum intensity (Eq. 10) was calculated for each soil class and for different magnitude intervals using the average normalized spectral curves for each subsoil class, and then related to geological condition rock (Eq. 11), providing a scaling factor for site effect that clearly represents an average amplification global affecting the entire spectrum. Table 8 displays the obtained results.

$$I_{A,B,C,D} = \int_{0.05}^{2.5} \overline{R.S_a\,(T)}\; dt \tag{10}$$

where the quantity with overbar under the integral denotes the average normalized spectral curve for each soil class SCA, SCB, SCC, SCD and for all magnitude intervals.

$$S_{B,C,D} = \frac{I_{B,C,D}}{I_A} \tag{11}$$

It is clear that the previously calculated average amplification $\mathrm{S_B}$, $\mathrm{S_C}$, and $\mathrm{S_D}$ take into account not only the amplification due to the increase in ordinates of soil spectra in comparison to rock spectra, but also a contribution due to the change in shape of these spectra when they are constrained to have the same ordinate at zero period. As is well known, average normalized spectra for increasingly softer soils differ from those for rock because the plateau expands and shifts to longer periods. This introduces the 'spectral shape ratio' (SR), a factor that only reflects the difference between spectral shapes (Rey et al. 2002). As a result, the calculated average amplification factors were divided by the "spectral shape ratio" (SR) values, which were calculated by dividing the area under the PSA/PGA-normalized new design spectra of each soil class by the area under the corresponding PGA-normalized new design spectrum for soil class SCA. Table 9 displays the obtained spectral shape ratios SR.

Using Eq. 12, the soil factors are calculated for each soil class and for different magnitude intervals with respect to the database's rock site. Table 10 displays the results obtained for soil classes SCB, SCC, and SCD, as well as all magnitude intervals for wms and mhs. Firstly, one can see that the soil factors obtained for wms ($M \leq 5.5$) are greater than those obtained for mhs ($M > 5.5$) for a given soil class. This result is related to the nonlinear behavior of soils observed in large magnitude earthquakes (mhs). Furthermore, for mhs ($M > 5.5$), the site factor rises from SCA (sf = 1.0) to SCC before falling precipitously for SCD. This decrease is due to the nonlinear behavior that is more prevalent in this type of soil. For wms ($M \leq 5.5$), soil behavior is assumed to be linear, which is why the site factor increases from SCA (sf = 1.0) to SCD.

The disparity in the results for the various magnitude intervals for the two types of seismicity is also noticeable. By closely examining Table 7, the low number of records (in bold) of class SCA and magnitude intervals of $6.5 < M \leq 7.0$ and $7.0 < M \leq 7.5$ with 14 and 6 respectively, and also of soil class SCD and magnitude intervals of $3.5 < M \leq 4.0$, $5.0 < M \leq 5.5$, $6.0 < M \leq 6.5$ and $7.0 < M \leq 7.5$ with 12, 10, 6 and 10 respectively, can explain the low values of the soil factors associated with these magnitude intervals.

Table 8 I_{Soil}/I_A ratios for soil classes SCB, SCC and SCD obtained for all magnitude intervals for wms and mhs

Soil Class	wms					mhs				
	3.5<M≤4	4<M≤4.5	4.5<M≤5	5<M≤5.5	Mean	5.5<M≤6	6<M≤6.5	6.5<M≤7	7<M≤7.5	Mean
SCB	0.89	1.50	1.65	1.6	1.43	1.53	1.46	1.25	1.11	1.34
SCC	1.32	2.46	1.94	2.79	2.13	2.12	1.90	1.44	1.39	1.71
SCD	1.06	3.47	2.97	3.28	2.70	2.01	1.10	1.46	0.92	1.38

$$SF_B = \frac{S_B}{SR_B}$$
$$SF_C = \frac{S_C}{SR_C} \quad (12)$$
$$SF_D = \frac{S_D}{SR_D}$$

where $SR_{B,C,D}$ and $S_{B,C,D}$ are given in Table (9) and (8) respectively.

Averaging over all magnitude intervals (MI_1) and magnitude intervals with a statistically representative number of records (MI_2) is used to calculate site factors. Furthermore, with no clear explanations, other than the low number of records of the magnitude classes that provided abnormally low site factors, it appears more prudent from a statistical standpoint to calculate the mean site factor for each soil class, as being the mean between the site factors corresponding to the two cases MI_1 and MI_2. Table 11 displays the calculated and recommended soil factors, as well as the comparison with the soil factors obtained by Pitilakis et al. (2013), which shows similar trend.

Figure 7 compares proposed elastic spectra (in black) to current Algerian seismic code elastic spectra (RPA99/2003 2003) in dashed black line, the recorded database (in grey), and the median acceleration spectra (solid white line), as well as the 84th (average plus one standard deviation, dashed white line) percentiles, for seismicity categories mhs (Fig. 7a, c, e, g) and wms (Fig. 7b, d, f, h). For mhs seismicity class ($M > 5.5$), the Algerian seismic code elastic spectra seems to be representative of the median acceleration spectra (solid white line) with a slight underestimation of the plateau for soil class SCC and SCD, and an overestimation for SCA soil class due to the constant factor equal to 1.25 in Eqs. 1–4.

For wms seismicity class ($M \leq 5.5$), the plateau of the Algerian seismic code elastic spectra shows a systematic shift towards higher periods, and lower spectral amplitudes mainly for SCC and SCD soil classes, inducing overestimations and underestimations of spectral accelerations in high and low period ranges, respectively.

Figure 8 show the comparison of the proposed type 2 spectra for pga = 0.05 g and 0.1 g, and type 1 spectra for pga = 0.20 g and 0.30 g, with the spectra proposed by Pitilakis et al. (2018), for soil classes SCA, SCB, SCC and SCD, developed in the framework of the ongoing revision of Eurocode 8.

For soil classes SCA (column 1 of Fig. 8) and SCB (column 2 of Fig. 8), the proposed type 2 and type 1 spectra matches well with spectra of Pitilakis et al. (2018) except for SC B2 which constant spectral acceleration plateau exhibits relatively high amplification.

For soil class SCC (column 3 of Fig. 8), the proposed spectra type 2 and type 1 envelop, from T = 0.1s and T = 0.15 s respectively, the SC C1, SC C2 and SC C3 spectra of Pitilakis et al. (2018), except the SC C3 spectrum which exhibit relatively high amplification for pga = 0.05 g, and upper corner period of the constant spectral acceleration range for pga = 0.20 g. The proposed amplification site factor for pga = 0.30 g appears significant compared to those of Pitilakis et al. (2018). This discrepancy, however, may be explained by the Pitilakis amplification factor's nonlinear effects, which cause it to drop as pga increases, whereas the suggested one is an average value for each spectrum type.

Table 9 Spectral shape ratios SR from this study

Soil Class	wms (M≤5.5)	mhs (M>5.5)
SCB	1.14	1.17
SCC	1.37	1.32
SCD	1.59	1.46

For soil class SCD (column 4 of Fig. 8), the proposed spectra type 2 and type 1 underestimate the site amplification factor of Pitilakis et al. (2018) for pga = 0.05 g and pga = 0.20 g, respectively; whereas, they match them well for pga = 0.10 g and pga = 0.30 g. The limited quantity of SCD soil class records in the Algerian strong motion database can explain these discrepancies.

Finally, Table 12 summarizes the appropriate parameter values for the proposed horizontal elastic spectra in Algeria. The frequency content described by the plateau T_B - T_C and the soil factor are the important parameters that influence the horizontal elastic spectrum. Figure 9 shows the proposed normalized design elastic response spectra for the two seismicity levels and four soil classes. It illustrates significant variations in elastic spectra developed for the two seismicity levelss. The first difference involves the T_B - T_C plateau, which swings toward the high periods in mhs but is dominated by the low periods in wms. The second difference is the spectrum amplitude related to site factors, which is less important in the case of mhs due to the effects of nonlinearities in soils subjected to strong seismic accelerations.

2 Conclusion

This paper investigated the performance of the current elastic response spectra defined in the Algerian RPA99/2003 (2003) provisions against a large dataset of strong motion records. Northern Algeria lies along the Africa-Eurasia plate boundary. It is one of the most seismically active areas in the western Mediterranean. The seismicity distribution, which ranges from strong to moderate in the north to moderate to low in the south, is represented by four (04) seismic zones. Because current elastic response spectra do not account for the various classes of seismicity and do not provide site factors for the four soil classes, their accuracy has been called into question in recent earthquakes.

The recent compilation of a large accelerometric database from Algeria and surrounding regions is used to improve the accuracy of the current elastic response spectra, as well as to develop new horizontal elastic acceleration response spectra and soil amplification factors for four soil classes (rock, firm, soft, and very soft soils) and two seismicity levels, weak to moderate seismicity (wms) for the central and southern regions and moderate to high seismicity (mhs) for the northern region.

The first step was to look into the limits of the constant spectral acceleration branch, which could be estimated by fitting the general form with experimental normalized acceleration response spectra. The results reveal that when the magnitude changes from wms (M $\leq$ 5.5) to mhs (M > 5.5), the limits of the constant spectral acceleration branch shift towards higher periods. This result supports our interest in proposing two types of spectra for the two seismicity classes.

The site effect is investigated by computing the soil factor of horizontal elastic response spectra using Housner spectrum intensity for soil classes SCB, SCC, and SCD at two seis-

Table 10 Soil factors for soil classes SCB, SCC and SCD obtained for all magnitude intervals for mhs and wms

Soil Class	wms					mhs				
	3.0<M≤4.0	4.0<M≤4.5	4.5<M≤5.0	5.0<M≤5.5	Mean	5.5<M≤6.0	6.0<M≤6.5	6.5<M≤7.0	7.0<M≤7.5	Mean
SCB	0.78	1.32	1.45	1.48	1.26[1] 1.42[2]	1.31	1.25	1.07	0.95	1.15[1] 1.28[2]
SCC	0.97	1.80	1.42	2.04	1.55[1] 1.75[2]	1.61	1.44	1.09	1.05	1.30[1] 1.52[2]
SCD	0.67	2.18	1.87	2.07	1.70[1] 2.04[2]	1.38	0.75	1.00	0.63	0.94[1] 1.38[2]

[1]Site factors are calculated by averaging over all magnitude intervals (MI_1);

[2]Site factors are calculated by averaging over magnitude intervals that have a statistically representative number of records (MI_2)

Table 11 Soil factors proposed by this study and comparison with those proposed by Pitilakis et al. (2013) and by RPA99/2003 (2003)

Seismicity category	Soil Class	This study			Recommended	Pitilakis et al. (2013)*	RPA99/2003 (2003)
		MI_1	MI_2	Average			
mhs M>5.5	SCA	1.0	1.0	1.0	1.0	1.0	1.0
	SCB	1.15	1.28	1.21	1.20	1.1–1.3 (1.20)	1.0
	SCC	1.30	1.52	1.41	1.40	1.7–1.3 −1.3 (1.43)	1.0
	SCD	–	1.38	1.38	1.35	1.8	1.0
wms M≤5.5	SCA	1.0	1.0	1.0	1.0	1.0	1.0
	SCB	1.26	1.42	1.34	1.35	1.2–1.5 (1.35)	1.0
	SCC	1.55	1.75	1.65	1.65	1.8–1.7–2.1 (1.86)	1.0
	SCD	1.70	2.04	1.87	1.85	2.0	1.0

*Pitilakis et al. (2013) proposes 2 and 3 subclasses for SCB and SCC respectively (the average value is given in brackets)

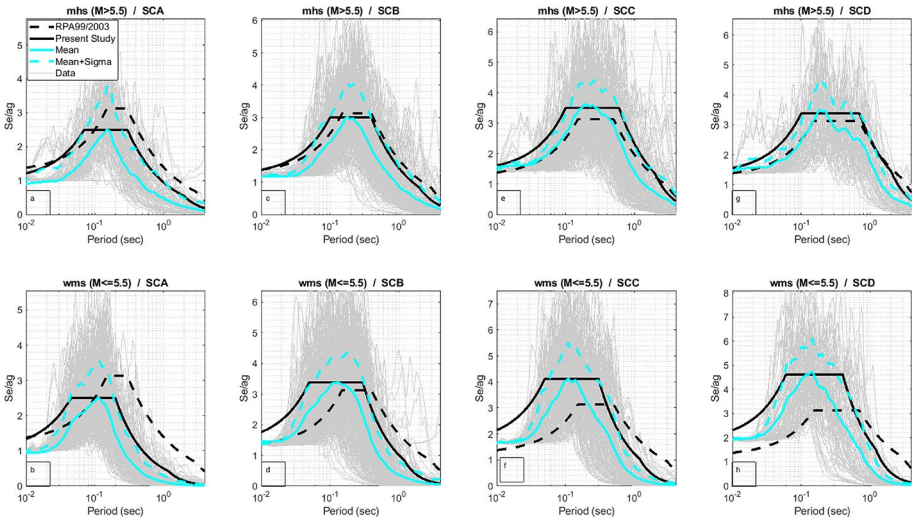

Fig. 7 Comparison between the proposed normalized elastic spectra (in black line), the current Algerian elastic spectra (RPA99/2003 (2003) in dashed black line), the recorded database (in grey), and the median acceleration spectra (solid green line), as well as the 84th (average plus one standard deviation, dashed green line) percentiles, for seismicity categories mhs (Fig. 5a, c, e, g) and wms (Fig. 5b, d, f, h)

micity levels (mhs and wms). The results indicate that the soil factors obtained for wms (M < 5.5) are higher than those obtained for mhs (M > 5.5). This finding is directly related to the nonlinear behaviour of soils during high seismic acceleration. Furthermore, comparing the proposed elastic acceleration spectra with the spectra provided by Pitilakis et al. (2018), developed in the framework of the ongoing revision of Eurocode 8, reveals comparable trends.

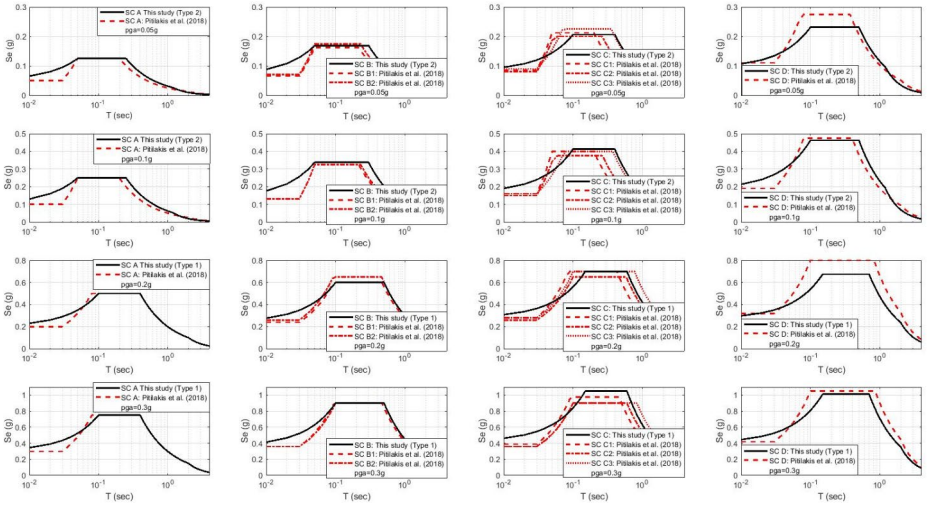

Fig. 8 Comparison of the proposed type 2 spectra for pga = 0.05 g and 0.1 g, and type 1 spectra for pga = 0.20 g and 0.30 g, with the spectra proposed by Pitilakis et al. (2018), for soil classes SCA, SCB, SCC and SCD

Table 12 Parameters values recommended for the proposed horizontal elastic spectra for Algeria

		mhs (M > 5.5)				wms (M ≤ 5.5)			
Parameters		T_B	T_C	α	S	T_B	T_C	α	S
Soil class	SCA	0.10	0.40	1	1	0.05	0.25	1	1
	SCB	0.10	0.50	1	1.20	0.05	0.30	1	1.35
	SCC	0.15	0.60	1	1.40	0.10	0.40	1	1.65
	SCD	0.15	0.70	1	1.35	0.10	0.50	1	1.85

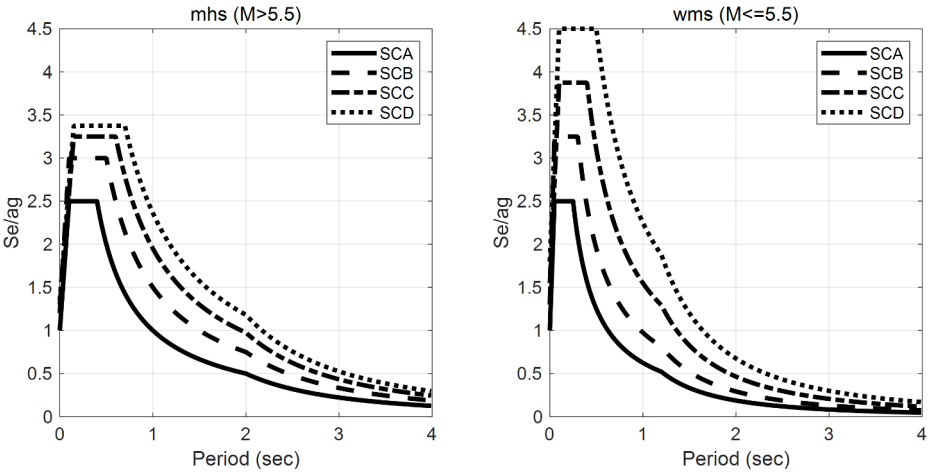

Fig. 9 Proposed design normalized elastic response spectra for the seismicity levels mhs and wms

Acknowledgements The authors thank CGS accelerograph network operators and the technical staff for rigorously maintaining the Algerian Accelerograph Network, especially Mr Haddouche Djamel. They thank also Mr Gherboudj Faouzi for proofreading the manuscript, as well as three anonymous reviewers for their valuable comments, effort and time allocated to improve the paper.

Author contributions All authors contributed to the study conception and design. Material preparation and data collection were performed by Laouami Nasser and Slimani Abdennasser. Numerical computation and analysis were performed by Laouami Nasser. The first draft of the manuscript was written by Laouami Nasser. Laouami Nasser commented and revised previous and actual versions of the manuscript. All authors read and approved the final manuscript.

Funding The authors declare that no funds, grants, or other support were received during the preparation of this manuscript.

Data availability The Algerian dataset analysed during the current study is available in the CGS repository, http://www.cgs-dz.org/index.php/fr/reseau-accelerometriques.

Declarations

Conflict of interest The authors have no relevant financial or non-financial interests to disclose.

References

Ambraseys NN, Simpson KA, Bommer JJ (1996) The prediction of horizontal response spectra in Europe. Earthquake Eng Struct Dynam 25:371–400

Ambraseys N, Smit P, Berardi R, Rinaldis D, Cotton F, Berge C (2000) Dissemination of European Strong Motion Data. CD-ROM collection. European Commission, Directorate XII, Environmental and Climate Programme, ENV4-CT97-0397. Brussel, Belgium

Bommer JJ, Acevedo AB (2004) The use of real earthquake accelerograms as input to dynamic analyses. J Earthquake Eng 8:43–91

Building Seismic Safety Council (BSSC) (1995) NEHRP recommended provisions for seismic regulations for new buildings. FEMA-222A/223A. Washington, D.C.

CEN (2004) Eurocode 8, design of structures for earthquake resistance—part 1: general rules, seismic actions and rules for buildings. EN 1998-1: 2004. Comite Europeen de Normalisation, Brussels

Deoda VR, Adhikary S (2020) A preliminary proposal towards the revision of Indian seismic code considering site classification scheme, amplification factors and response spectra. Bull Earthq Eng 18:2843–2889

Harmon J, Hashash YMA, Stewart JP, Rathje EM, Campbell KW, Silva WJ, Ilhan O (2019a) Site amplification functions for Central and Eastern North America—part II: modular simulation-based models. Earthq Spectra 35:815–847

Harmon J, Hashash YMA, Stewart JP, Rathje EM, Campbell KW, Silva WJ, Xu B, Musgrove M, Ilhan O (2019b) Site amplification functions for Central and Eastern North America—part I: simulation data set development. Earthq Spectra 35:787–814

Housner GW (1959) Behavior of structures during earthquakes. J Eng Mech Div 85:109–129

Laouami N (2020) Proposal for a new site classification tool using Microtremor data. Bull Earthq Eng 18:4681–4704. https://doi.org/10.1007/s10518-020-00882-4

Laouami N, Slimani A, Larbes S (2018a) Ground motion prediction equations for Algeria and surrounding region using site classification based H/V spectral ratio. Bull Earthq Eng. https://doi.org/10.1007/s10518-018-0310-3

Laouami N, Hadid M, Mezouar N (2018b) Proposal of an empirical site classification method based on target simulated horizontal over vertical spectral ratio. Bull Earthq Eng 16:5843–5874. https://doi.org/10.1007/s10518-018-0420-y

Moradpouri F, Mojarab M (2012) Determination of horizontal and vertical design spectra based on ground motion records at Lali tunnel, Iran. Earthq Sci 25(4):315–322

Newmark NN, Hall WJ (1982) Earthquake spectra and design. Earthquake Engineering Research Institute, Berkeley

Pitilakis K, Riga E, Anastasiadis A (2013) New code site classification, amplification factors and normalized response spectra based on a worldwide ground-motion database. Bull Earthq Eng 11:925–966. https://doi.org/10.1007/s10518-013-9429-4

Pitilakis K, Riga E, Anastasiadis A, Fotopoulou S, Karafgka S (2018) Towards the revision of EC8: proposal for an alternative site classification scheme and associated intensity dependent spectral amplification factors. Soil Dyn Earthq Eng. https://doi.org/10.1016/j.soildyn.2018.03.030

Rey J, Faccioli E, Bommer JJ (2002) Derivation of design soil coefficients (S) and response spectral shapes for Eurocode 8 using the European strong-motion database. J Seismol 6:547–555.

RPA99/2003 (2003) Règlement Parasismique Algérien. CGS Earthquake Engineering Research Center, Algiers

Yang J, Lee CM (2007) Characteristics of vertical and horizontal ground motions recorded during the Niigata-ken Chuetsu, Japan earthquake of 23 october 2004. Eng Geol 94(1):50–64

Authors and Affiliations

Nasser Laouami[1] · Abdennasser Slimani[1]

✉ Nasser Laouami
nlaouami@cgs-dz.org

Abdennasser Slimani
aslimani@cgs-dz.org

[1] Centre National de Recherche Appliquée en Génie Parasismique, BP.232 Hussein Dey, 16040 Algiers, Algeria